EPJ Web of Conferences **164**, 06002 (2017) DOI: 10.1051/epjconf/201716406002
ICNFP 2016

Nucleon structure observables with $\overline{\text{P}}$ANDA

María Carmen Mora Espí[1,2,a],
on behalf of the $\overline{\text{P}}$ANDA collaboration

[1] *Institut für Kernphysik, Johannes Gutenberg-Universität Mainz, Johann-Joachim-Becher-Weg 45, D-55128 Mainz, Germany.*
[2] *Helmholtz-Institut Mainz, Staudingerweg 18, 55128 Mainz, Germany.*

Abstract. The $\overline{\text{P}}$ANDA detector will be built as a part of the future FAIR facility in Darmstadt. The availability of an antiproton beam with beam momenta up to 15 GeV/c will make possible a broad nuclear physics program. Topics like hadron spectroscopy in the charmonium mass region, the property of hadrons inside nuclear matter, hypernuclear physics, or nucleon properties using electromagnetic processes are part of the physics program of $\overline{\text{P}}$ANDA. The main part of this contribution concentrates on the feasibility of measurement of nucleon structure observables, such as electromagnetic form factors or transition distribution amplitudes, via experiments using electromagnetic processes in $\overline{\text{P}}$ANDA.

1 Introduction

Understanding Quantum Chromodynamics (QCD), describing the strong force, is one of the most challenging fields of physics. The interaction mechanisms between fundamental particles can be described using perturbative QCD (p-QCD) at short distances with very high precision and predictive power. However, at long distances a series of spectacular phenomena, *e.g.* generation of hadron masses, formation of hadronic matter and color confinement, appear, and these cannot be described by basic QCD principles. The ultimate goal for the $\overline{\text{P}}$ANDA (anti$\overline{\text{P}}$roton ANnihilations at DArmstadt) experiment will be to explore the strong interaction at precisely the energy interval corresponding to the transition between the perturbative and the non-perturbative regimes of QCD. The high-intensity and high-resolution antiproton beam of the High Energy Storage Ring (HESR), ranging from $p_{\bar{p}} = 1.5$ GeV/c to $p_{\bar{p}} = 15$ GeV/c, of the future Facility for Antiproton and Ion Research (FAIR) in Darmstadt will be an excellent instrument to fulfill the ambitious physics program foreseen by the $\overline{\text{P}}$ANDA collaboration [1]. This includes several fields of research:

- **Hadron spectroscopy**: The study of QCD bound states (charmonium, *D*-meson and baryon spectroscopy, exotic states...) is of fundamental importance for a better, quantitative understanding of QCD. Unique precision measurements will help to distinguish between the different theory approaches used for the computation of particle spectra. The study of exotic bound states such as glueballs or hybrids will be also addressed in the $\overline{\text{P}}$ANDA collaboration.

[a] e-mail: mamoraes@uni-mainz.de

- **Hyperon production dynamics**: The measurement of reactions involving hyperons can help studying the creation mechanism of quark-antiquark pairs and their arrangement to hadrons. The self-analysing weak decays of most hyperons give access to spin degrees of freedom for these reactions.
- **Study of Hadrons in Nuclear Matter**: The study of medium modifications of hadrons embedded in hadronic matter is aimed at understanding the origin of hadron masses in the context of spontaneous chiral symmetry breaking in QCD and its partial restoration in a hadronic environment.
- **Hypernuclear Physics**: The availability of antiproton beams at FAIR will allow efficient production of hypernuclei with more than one strange hadron. In particular, the production of Ξ can be used to form double Λ hypernuclei, which will offer a unique opportunity to study basic properties of the potential between nucleons and hyperons in a bound state.
- **Electroweak Physics**: With the high intensity antiproton beam available at HESR, a large number of D-mesons can be produced. This gives the possibility to observe rare weak decays of these mesons allowing studying electroweak physics by probing predictions of the Standard Model and searching for enhancements introduced by processes beyond the Standard Model.
- **Nucleon structure**: $\overline{\text{P}}$ANDA will enable the investigation of the structure of the nucleon using electromagnetic processes. Nucleon structure observables, *e.g.* the Electromagnetic Form Factors (EMFF) or the Transition Distribution Amplitudes (TDA) will be measured with $\overline{\text{P}}$ANDA. Detailed information about these and other processes are presented later in this paper.

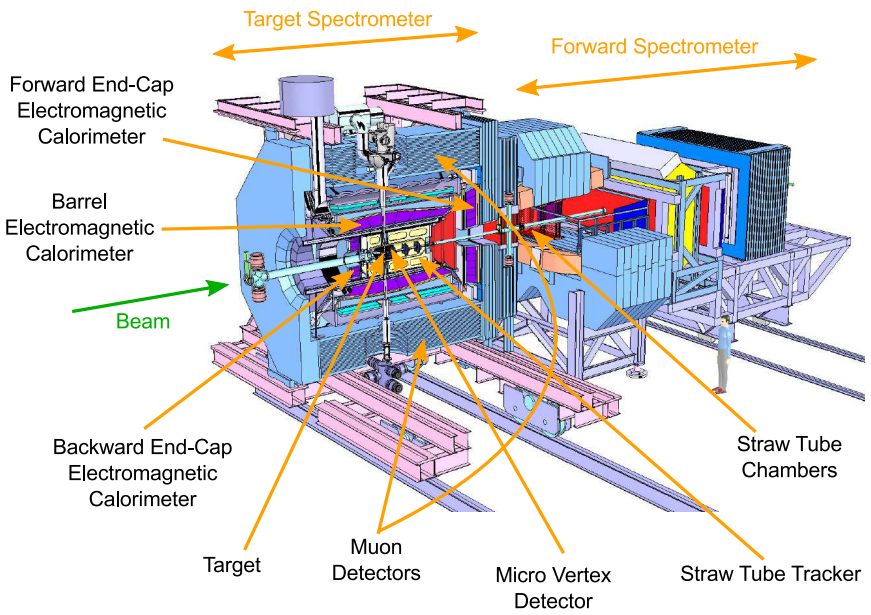

Figure 1. Sketch of the $\overline{\text{P}}$ANDA detector, divided into the target spectrometer and the forward spectrometer. Both spectrometers contain modular detectors for tracking, particle identification, electromagnetic calorimetry and muon identification. The main detectors in the target spectrometer are signaled with arrows.

In order to successfully achieve the previously mentioned goals, $\overline{\text{P}}$ANDA needs to be an almost 4π detector with very good energy resolution, at a few percent level, and excellent particle identification (PID) capabilities, with a fast data acquisition system (DAQ) and high radiation hardness. The basic

concept of the setup is a fixed-target experiment divided into a target spectrometer, with a 2 T solenoid around the target area to detect particles with low momenta, and a forward spectrometer based on a 2 T dipole in order to ensure particle detection below 2° for faster particles. Modular detectors for tracking, particle identification, electromagnetic calorimetry and muon identification are designed for both spectrometers. The modularity will enable an easy replacement of parts of the tracking system and the backward Electromagnetic Calorimeter (EMC) with the hypernuclear setup. The latter has dedicated targets and gamma-ray detectors that will be used in a more advanced stage of the measurement program. Figure 1 shows a sketch of the $\overline{\text{P}}$ANDA detector depicting various subsystems foreseen to achieve the desired detection capabilities. A complete description of the different setups can be found in various technical design reports [2–7].

2 Nucleon structure observables

2.1 Proton Electromagnetic Form Factors

The annihilation of $\bar{p}p$ into an e^+e^- pair (or more generally, a $\ell^+\ell^-$ pair, with $\ell = e,\ \mu$) via a virtual photon of mass $q^2 = s$ (with s being the squared total energy available in the annihilation) gives access to the hadron-electromagnetic vertex $\gamma^\star \bar{p}p$. This vertex gives information about the proton EMFF, *i.e.* analytical functions of q^2 parameterizing the hadronic current at the vertex. The kinematic region accessible by $\overline{\text{P}}$ANDA is the time-like (TL) region of momentum transfer squared, $q^2 > 0$, also reachable by the time-reversed reaction $e^+e^- \to \bar{p}p$ (in general, $\ell^+\ell^- \to \bar{p}p$). This reaction is related by crossing symmetry to elastic electron-proton scattering (see Fig. 2), which gives access to the space-like (SL) region of momentum transfer squared, $q^2 < 0$. In the SL region, the EMFF can be interpreted as the Fourier transform of the distribution of charge and magnetization in the Breit-frame. Both regions are connected due to the analyticity and unitarity of the EMFF via the dispersion relations. A full review on EMFF can be found for example in Ref. [8].

The proton EMFF in the SL region have been studied since many years and abundant and precise data exist in this region. However, recent analyses using polarization methods show results in contradiction with older results from Rosenbluth separation. This has given rise to a lot of discussion about the knowledge of the SL EMFF. In addition, the data collected in the TL region are still very limited. Any measurement here would contribute to expand the knowledge on these functions, not only in the TL region but also in the SL region. The $\overline{\text{P}}$ANDA experiment will offer an excellent opportunity to extend the, until now, scarce data bank on TL EMFF, and therefore will help disentangling the questions arisen about the EMFF in the last years (see also Refs. [9, 10]).

The current world-wide data available on the EMFF in the TL region are shown in Fig. 3. Due

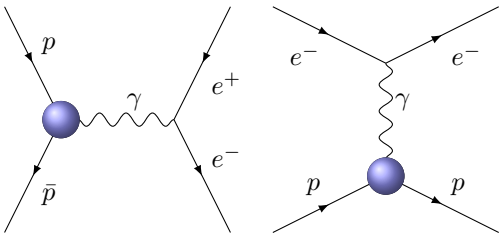

Figure 2. Feynman diagrams of the reactions $\bar{p}p \to e^+e^-$ and $e^-p \to e^-p$. The balls represent the hadron electromagnetic vertex. Both diagrams are connected by crossing symmetry.

to the small data samples, only the measurement of the ratio R or the measurement of an effective form factor under the assumption $|G_E| = |G_M|$ was possible. The results extracted by BaBar [11], from measurements of initial state radiation (ISR) processes ($e^+e^- \to \bar{p}p\gamma$) are not in agreement with the previous results from LEAR ($\bar{p}p \to e^+e^-$) [12]. More recent measurements by BESIII [13] at different energies using $e^+e^- \to \bar{p}p$ have large uncertainties. Other measurements do not add more relevant information [14, 15]. It is clear that the puzzle of the EMFF in the TL region is far from being understood. The high intensity and high resolution beam of $\overline{\mathsf{P}}$ANDA will enable the measurement of the differential cross section of the process $\bar{p}p \to e^+e^-$, which will grant not only the ratio between $|G_E|$ and $|G_M|$, but also the chance to separate them. Feasibility studies for the measurement of the TL EMFF with $\overline{\mathsf{P}}$ANDA using the reactions $\bar{p}p \to e^+e^-$ and $\bar{p}p \to \mu^+\mu^-$ have been performed and are summarised in the following.

Concerning the studies for the reaction $\bar{p}p \to e^+e^-$ [16], two independent simulations were performed. Method-I makes use of a dedicated event generator based on the theoretical cross section [17],

$$\frac{d\sigma}{d\cos\theta} = \frac{\pi\alpha^2}{8EP}\left[|G_M|^2(1+\cos^2\theta) + \frac{|G_E|^2}{\tau}(1-cos^2\theta)\right], \tag{1}$$

with E and P are the energy and momentum of the antiproton in the center of mass (CM) frame, α is the fine structure constant, $\tau = \frac{q^2}{4M_p^2}$, and θ is the lepton emission polar angle in the proton-antiproton CM system. In these simulations, $|G_E|/|G_M| = 1$ is assumed, and the expected amount of events is generated at each energy. In Method-II, 10^6 events are simulated using a flat angular distribution and the results are later scaled to the expected size of the data sample using a given model (*i.e.* Eq. 1 with $|G_E| = |G_M|$). In both methods an independent simulated sample with 10^6 events is used for the study of the efficiency. In Method-I, a fit using the cross section formula in Eq. 1 to the reconstructed, efficiency corrected distribution, as a function of $\cos^2\theta$ is used to extract the values of the EMFF. In Method-II, a linear fit to

$$y = \sigma_0 + \sigma_0\mathcal{A}\cos^2\theta\,, \tag{2}$$

with

$$\sigma_0 = \frac{\pi\alpha^2}{2\beta s}\left(|G_M|^2 + \frac{1}{\tau}|G_E|^2\right) \text{ and } \mathcal{A} = \frac{\tau - R^2}{\tau + R^2}, \tag{3}$$

is used. The main challenge of this analysis is the elimination of the huge hadronic background, due to the 10^6 times larger cross section of the channel, $\bar{p}p \to \pi^+\pi^-$. For the studies of the suppression of the main background channel, an event generator based on the calculations in Ref. [18] was developed in Mainz [19]. Other channels (*e.g.* $\bar{p}p \to K^+K^-$) are easily suppressed using kinematic constraints.

Both simulations arrive to the same conclusion: $\overline{\mathsf{P}}$ANDA will be able to measure the ratio between the electric and magnetic Form Factors (FF), $R = |G_E|/|G_M|$ in a broad range of q^2 values up to $q^2 = 14\,(\mathrm{GeV/c})^2$, improving the precision of the existing results in at least one order of magnitude. In addition, the separation between the electric and magnetic FF will be possible. The measurement of the proton effective FF can be extended to higher q^2 values according to the experimental efficiency. The results of these simulations are shown in Tab. 1 and Tab. 2, and also in Fig. 3 together with the results from previous experiments.

The difference between the error bars extracted with each method at $q^2 = 13.9\,\mathrm{GeV/c^2}$ is explained by the different size of the data samples considered in each simulation. Given an integrated luminosity of $2\,\mathrm{fb}^{-1}$, Method-I takes into account the expected number of events for the simulation at each energy, considering thus the statistical fluctuations within the data sample, whereas Method-II smears this effect by simulating higher statistics and then rescaling to the same amount of events used in the

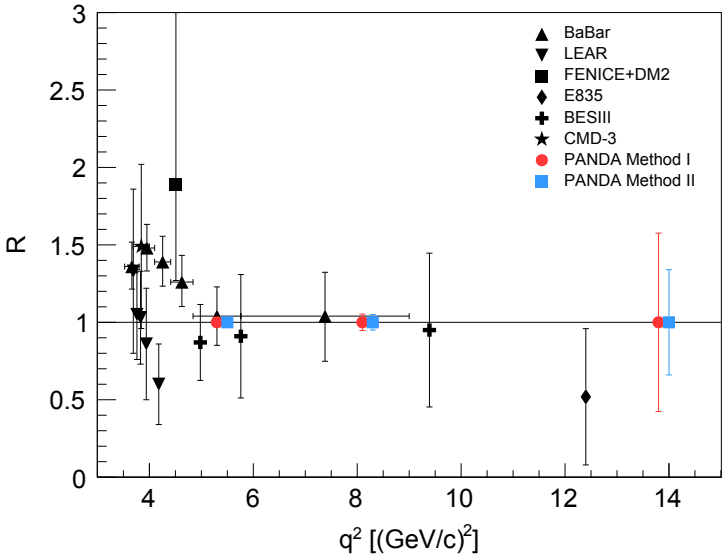

Figure 3. Expected statistical precision on the determination of the proton FF ratio from the simulations as reported in Ref. [16] (blue squares and red circles) for $R = 1$ as a function of q^2, compared with the existing data. Data are from references [11–15].

Table 1. Expected uncertainties for the measurement of the $|G_E|$, $|G_M|$ and the ratio R (Method-I). For more information, we refer to Ref. [16].

q^2 [(GeV/c)^2]	$\Delta\|G_E\|/\|G_E\|$ [%]	$\Delta\|G_M\|/\|G_M\|$ [%]	$\Delta R/R$ [%]
5.4	2.2	3.5	3.3
8.2	5.4	2.6	6.6
13.9	48	9.7	57

Table 2. Expected uncertainties for the measurement of the ratio R and the angular asymmetry on the proton FF (Method-II). For more information, we refer to Ref. [16].

q^2 [(GeV/c)^2]	R	ΔR	$\mathcal{A}$	$\Delta\mathcal{A}$
5.40	1	0.014	0.210	0.014
8.21	1	0.050	0.400	0.042
13.9	1	0.407	0.590	0.264

first simulation. The error bars of Method-II represent the most probable uncertainty if the measurement is done only once. That means, repeating the experiment multiple times and plotting the error distribution, we should get a Gaussian distribution with a sigma equal to the uncertainty extracted by Mehtod-II. This was confirmed by repeating the simulation using Method-I several times and fitting the distribution of errors from the single simulations. Taking this into account, in Method-II the un-

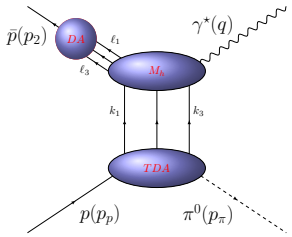

Figure 4. Feynman diagram of the process $\bar{p}p \to \gamma^\star\pi^0 \to e^+e^-\pi^0$. This process can be measured in $\overline{\text{P}}$ANDA to access the TDA.

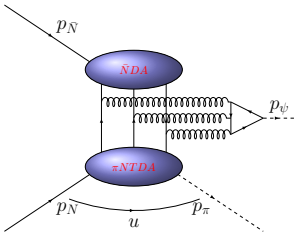

Figure 5. Feynman diagram of the process $\bar{p}p \to \pi^0 J/\psi$. This process can be measured in $\overline{\text{P}}$ANDA to access the TDA.

certainty expected in $\overline{\text{P}}$ANDA is extracted, while the results of Method-I show just one possible value for the error bars.

With $\overline{\text{P}}$ANDA it will be also possible to determine for the first time the EMFF through the reaction $\bar{p}p \to \mu^+\mu^-$ [20]. For this channel the cross section and the background to signal ratio considerations are the same as for the electron channel. The measurement with muons will be useful to verify the results obtained with the measurement of $\bar{p}p \to e^+e^-$ and to study the systematic effect in the electron channel due to higher order radiative corrections from the final state. The suppression of the main background channel, $\bar{p}p \to \pi^+\pi^-$, is more difficult in this case due to the similar masses of pions and muons. Simulations of the signal and background channels have been performed with the same dedicated event generators described for the simulations discussed earlier. Following a similar strategy, by applying a set of cuts on kinematical variables and detector observables combined with a vertex fitting, the desired background suppression for this measurement cannot be reached. A method based on a multivariate data classification delivers a huge improvement with respect to the simple analysis based on hard cuts. A signal to background ratio of 1:4 is achieved, in comparison to the previously reached 1:30. At this level of contamination, a background subtraction based on the previously measured background channel can be applied. An independently generated background sample was used to study how the background substraction has to be performed. For a beam momentum of $p_{\bar{p}} = 1.7\,\text{GeV/c}$, a statistical precision of $\Delta|G_E|/|G_E| \sim 8.6\,\%$, $\Delta|G_M|/|G_M| \sim 4.1\,\%$ and $\Delta R/R \sim 5.1\,\%$ can be achieved.

2.2 Transition Distribution Amplitudes

TDA are parameterizations of the hadronic matrix elements that occur in perturbative QCD calculations of a certain family of reactions within the framework of collinear factorization. The cross

section of this processes can be divided into a perturbative part, calculable thanks to the high momentum transferred in the process, and a non-perturbative, but universal and measurable part, which is described by TDA. In particular, with $\overline{\text{P}}$ANDA, the study of π-NTDA will be possible via the proposed mechanism reported in Ref. [21], by measuring the cross section of $\bar{p}p \to \gamma^\star\pi^0 \to e^+e^-\pi^0$ with the emission of the π^0 in the very forward or backward limit (see Fig. 4). This constraint is necessary in order to ensure the hard scale in which the perturbative expansion of the hard subprocess is applicable. Feasibility studies to access the π-NTDA following the cross section calculations in Ref. [21] have been described in Ref. [22]. The study of the channel $\bar{p}p \to \pi^0 J/\psi$, shown in Fig. 5, is a natural complement to the first analysis due to its higher cross section and because it can also be used to access the TDA. Therefore, it has been analysed in Ref. [23]. The measurement of these channels with $\overline{\text{P}}$ANDA will represent a test of QCD factorization, and the validity and universality of the TDA approach. For the first channel ($\pi^0\gamma^\star$), simulations were performed at two values of the CM energy squared, s. The cross section can be determined with an accuracy $\Delta\sigma/\sigma$ between 12 % to 24 %. The studies for the second channel $\bar{p}p \to \pi^0 J/\psi$, have been performed at three different values of s. The results show a background contamination lower than 1 %, coming from the channels $\bar{p}p \to \pi^0\pi^+\pi^-$, $\bar{p}p \to \pi^0\pi^+\pi^+\pi^-\pi^-$, $\bar{p}p \to \pi^0\pi^0\pi^+\pi^-$, $\bar{p}p \to \pi^0\pi^0 J/\psi$, and $\bar{p}p \to \pi^0\gamma^\star \to e^+e^-$, with a signal efficiency reconstruction of about 5 % to 10 %.

2.3 Other structure functions

The physics program of $\overline{\text{P}}$ANDA also comprises the measurement of other structure functions as *e.g.* the Generalized Distribution Amplitudes (GDA) and the Transverse Momentum Dependent Parton Distribution Functions (TMD-PDF). The GDA are the TL counterparts of the Generalized Parton Distributions (GPD) which are measured in the SL region via Wide Angle Compton Scattering (WACS) in reactions like $\gamma p \to \gamma p$. With $\overline{\text{P}}$ANDA, the reactions $\bar{p}p \to \gamma\gamma$ and $\bar{p}p \to \gamma\pi^0$ can be used for probing the GDA. Preliminary studies [1] show that it will be possible to achieve a signal to background ratio between 1 and 2 and efficiencies ranging between 25 % and 50 %.

TMD-PDF are experimentally very well known functions in the SL region. $\overline{\text{P}}$ANDA will shed light on of these functions in the TL region. In particular they can be measured via Drell-Yan (DY) processes. Preliminary studies [1, 24] show a production of DY processes of the order of $1.3 \cdot 10^5$ DY/month with a reconstruction efficiency of ca. 33 %. More studies on the measurement of these functions are nevertheless needed to determine the real potential of $\overline{\text{P}}$ANDA in this area.

2.4 Summary

A series of feasibility studies for the measurement of different structure functions with the $\overline{\text{P}}$ANDA detector have been presented. The measurement of the EMFF in the TL region using the reaction $\bar{p}p \to e^+e^-$ will represent the most precise measurement so far done of these observables. The precision will be improved in at least one order of magnitude with respect to *e.g.* BaBar. In addition $|G_E|$ and $|G_M|$, will be measured separately. $\overline{\text{P}}$ANDA will also perform pioneering measurement of the EMFF using the reaction $\bar{p}p \to \mu^+\mu^-$, for the verification of the measurements made using electrons and to study the asymmetries introduced by radiative corrections.

The measurement of the TDA has been studied for two different reactions $\bar{p}p \to \gamma^\star\pi^0$ and $\bar{p}p \to J/\psi\pi^0$, and the results are very promising.

Other nucleon structure observables, such as GDA and TMD-PDF, are also considered to be measured with $\overline{\text{P}}$ANDA and the preliminary results are encouraging.

Among these measurements, $\overline{\text{P}}$ANDA will produce results on charmonium spectroscopy, hypernuclear physics, electroweak interactions, and it will be able to study hadrons in a nuclear medium.

In conclusion, $\overline{\text{P}}$ANDA will be an excellent experiment for the expansion of the knowledge on nuclear physics and QCD.

3 Acknowledgments

This work was supported by the Bundesministerium für Bildung und Forschung (BMBF) through grant 05P12UMFP9.

References

[1] W. Erni et al. (PANDA) (2009), arXiv:0903.3905
[2] W. Erni et al. (PANDA) (2008), FAIR TDR 4-01, arXiv:0810.1216
[3] W. Erni et al. (PANDA) (2009), FAIR TDR 4-02, arXiv:0907.0169
[4] W. Erni et al. (PANDA) (2012), FAIR TDR 4-03, arXiv:1207.6581
[5] W. Erni et al. (PANDA), Eur. Phys. J. **A49**, 25 (2013), FAIR TDR 4-04
[6] W. Erni et al. (PANDA) (2013), FAIR TDR 4-05
[7] W. Erni et al. (PANDA) (2014), FAIR TDR 4-06
[8] S. Pacetti, R. Baldini Ferroli, E. Tomasi-Gustafsson, Phys. Rept. **550-551**, 1 (2015)
[9] E. Tomasi-Gustafsson, M.P. Rekalo (2008), arXiv:0810.4245
[10] E. Tomasi-Gustafsson et al., Eur. Phys. J. **A24**, 419 (2005)
[11] J.P. Lees et al. (BaBar), Phys. Rev. **D88**, 072009 (2013)
[12] G. Bardin et al., Nucl. Phys. **B411**, 3 (1994)
[13] M. Ablikim et al. (BESIII), Phys. Rev. **D91**, 112004 (2015)
[14] R.R. Akhmetshin et al. (CMD-3), Phys. Lett. **B759**, 634 (2016)
[15] R. Baldini et al., Eur. Phys. J. **C46**, 421 (2006)
[16] B. Singh et al. (PANDA), Eur. Phys. J. **A52**, 325 (2016)
[17] A. Zichichi et al., Nuovo Cim. **24**, 170 (1962)
[18] J. Van de Wiele, S. Ong, Eur. Phys. J. **A46**, 291 (2010)
[19] M. Zambrana et al. (2012), PANDA Internal Note
[20] I. Zimmermann, A. Dbeyssi, D. Khaneft (PANDA), AIP Conf. Proc. **1735**, 080004 (2016)
[21] J.P. Lansberg, B. Pire, L. Szymanowski, Phys. Rev. **D76**, 111502 (2007)
[22] B.P. Singh et al. (PANDA), Eur. Phys. J. **A51**, 107 (2015)
[23] B. Singh et al. (PANDA) (2016), arXiv:1610.02149
[24] M. Destefanis (PANDA), EPJ Web Conf. **73**, 02012 (2014)